Electrical-Distance-Based Preselection of Candidate Sites for Reactive Power Planning

Soupayan Bose, Reinaldo Tonkoski, Rolf Witzmann
Chair of Electric Power Transmission and Distribution
Technical University of Munich
Munich, Germany
soupayan.bose, reinaldo.tonkoski, rolf.witzmann@tum.de

Mojtaba Momeni, Jörg Michael Schmidt
Energy System Planning — System Integrity
TenneT TSO GmbH
Bayreuth, Germany
Mojtaba.Momeni, JoergMichael.Schmidt@tennet.eu

***Abstract*—With a decreasing number of synchronous machines in modern power systems, dynamic reactive power support is a concern in transmission system planning. Dynamic reactive power planning for short-term voltage stability generally relies on time-domain simulations, which are computationally expensive, especially for large grids. Exploiting the local nature of the impact of reactive power on voltages, this paper proposes distance-based methods for preselection of candidate buses to reduce the computational effort in such planning. Applied to a reduced model of the German transmission grid, within one control region, comparable results for optimised reactive power compensation were obtained with up to 85% reduction in simulation time.**

***Index Terms*—Reactive power planning, topological reduction, electrical-distance, reactive power compensation**

I. Introduction

The shift towards more converter-driven generation reduces the available dynamic reactive power in transmission grids, conventionally sourced from synchronous generators, while its demand simultaneously increases due to higher generation variability, the growing prevalence of converter-based loads, and higher grid utilisation [1]. Increased utilisation of the grid is also recommended in Germany [2] using methods such as dynamic line rating and use of high current conductors, which might further impact this demand.

Reactive power planning (RPP) methods considering short-term voltage stability commonly rely on trajectory sensitivities, which are often evaluated numerically using time-domain simulations [3]–[7]. Although this approach involves greater computations than directly solving the underlying differential–algebraic equations, it offers practical implementation advantages [3].

A previous work (DYNQ) [8] adopted a similar approach, based on the algorithm of [6], to determine an optimal dynamic reactive power compensation plan for a given grid considering multiple projected operating scenarios and fault cases. While effective, the method requires extensive time-domain simulations, resulting in computation times up to several days even for application to a single control region in Germany. Since the number of simulations scales directly with the number of candidate locations, applying it to larger grids would only increase the time-burden. This work introduces topology-aware, electrical-distance-based preselection of candidates to address this issue. This reduces the number of simulations, and consequently, the total computation time.

The rest of the paper is organised as follows. Section II explains the proposed methods for distance-based preselection of candidates. Section III then describes the simulation setup. Section IV discusses results with and without the candidate preselection methods, showing the improvements upon the original brute-force algorithm of DYNQ. Section V concludes the paper, along with the future outlook for this work.

The authors would like to thank TenneT TSO GmbH for funding this work.

II. Distance-Based Preselection of Candidates

The DYNQ algorithm relies on brute-force RMS simulations to compute voltage sensitivities to reactive power injections at each bus, making its computational effort directly proportional to the number of candidate buses. However, since voltage is a local phenomenon and reactive power injection only influences voltages in its electrical vicinity, distance-based candidate preselection is envisaged to reduce the simulation effort. Two methods are proposed. Candidate shortlisting selects buses close to violations, while candidate clustering groups buses close to each other and computes sensitivities once per group. The overall concept is illustrated in Fig. 1. The remainder of this section first provides a brief overview of the DYNQ framework, forming a basis for the current work, and then presents the proposed methods for distance-based preselection.

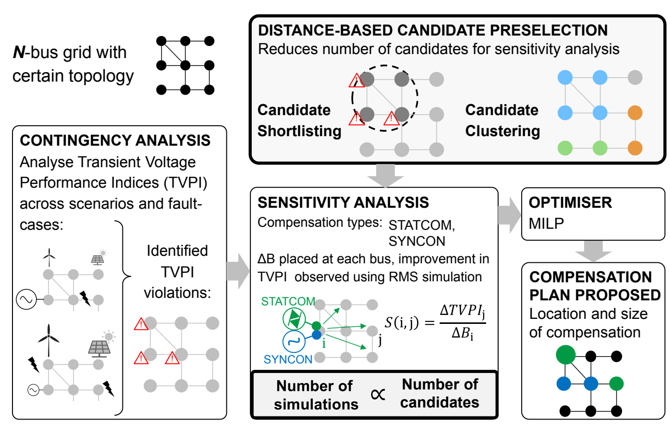

Fig. 1. Workflow of proposed candidate preselection to reduce the number of simulations required in DYNQ.

979-8-3315-8138-1

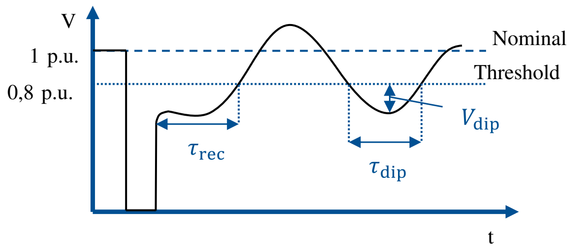

Fig. 2. Transient Voltage Performance Indices (TVPI).

A. The DYNQ Framework

The DYNQ (DYNamic-Q) toolbox is a Python-based framework that interfaces with PowerFactory [9] to systematically identify optimal sizing and placement of dynamic reactive power compensation to improve short-term voltage stability in transmission grids. This is done considering multiple predefined fault cases over a horizon of projected operating scenarios representing different hours of operation obtained from a year-round simulation. Static Synchronous Compensators (STATCOMs) and Synchronous Condensers (SYNCONs) are considered as candidate technologies [1].

The post-fault voltage recovery is quantified at each bus using three indices, namely, voltage recovery time (τ_{rec}), voltage dip magnitude (V_{dip}), and voltage dip duration (τ_{dip}), as shown in Fig. 2. These Transient Voltage Performance Indices (TVPI) capture the key features of delayed voltage recovery and oscillatory dynamics following a disturbance [10]. Buses violating predefined TVPI thresholds are flagged as Base-Out-of-Bound (BOB) Buses. DYNQ works on a substation level, where all busbars within a substation are assumed interconnected. The terms bus and substation are therefore used interchangeably.

Sensitivities are calculated by sequentially placing small test devices at each bus and observing the resulting TVPI changes across the grid through RMS simulations. These sensitivities feed into the Mixed-Integer Linear Program (MILP) optimiser that identifies the least-cost combination of STATCOMs and SYNCONs to eliminate all violations. To account for the linearisation assumption, the procedure is repeated iteratively, implementing the suggested incremental solution in the grid model after each iteration and verifying with RMS simulation, if all the violations have in fact been eliminated. The process continues until the cumulative solution resolves all violations under RMS verification.

The computational burden is largely dictated by the brute-force sensitivity calculations. The number of simulations required per iteration is given by (1), where D is the number of different types of compensation devices, K is the number of contingencies and $I \leq N$ is the number of candidate buses for installation of a compensation device in an N-bus grid.

$$NSIM_{sens} = D \cdot K \cdot I \tag{1}$$

By default, all N buses are both observed and candidates for placement of a compensation device. This work aims to reduce the computation effort by decreasing the number of candidate buses (I) through topology-aware preselection.

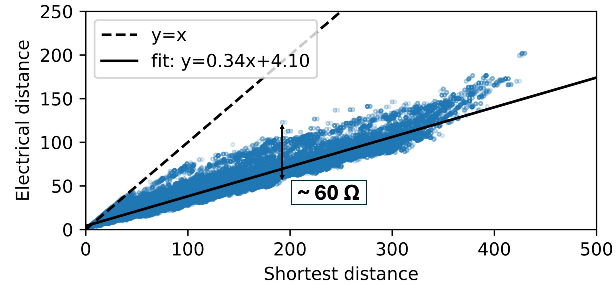

Fig. 3. Comparison of electrical distances with shortest-path distances

B. Topology-Extraction and Electrical Distances

The proposed approach first requires a representation of the grid topology, comprising all buses and connecting lines. The grid topology is reconstructed as a non-directional impedance-graph using NetworkX [11]. Given the high X/R ratios of EHV-grids [12], only the magnitude of impedances can be considered as weights. This is convenient, since several NetworkX algorithms operate on real-valued edge weights.

Effective electrical distances, considering parallel paths in a meshed grid, are calculated using NetworkX based on the algorithm presented in [13]. Fig. 3 compares electrical distances to shortest-path distances between node-pairs. It is interesting to observe a linear trend, despite notable deviations for many node-pairs. Electrical distances are therefore used to reflect the electrical connectivity between buses more accurately.

In hybrid AC–DC systems, the distance calculations, as well as the preselection methods, can be applied considering only the AC grid. Since DC lines do not provide a reactive power flow path, they are not expected to affect the effectiveness of the proposed distance-based preselection in an otherwise interconnected AC grid.

C. Distance-Based Shortlisting of Candidates

Since voltage is a local phenomenon, reactive power injection mainly affects voltages within its electrical vicinity. Candidate locations are therefore restricted to buses within a search radius of any BOB–bus. This defines a threshold on electrical distance, beyond which the influence of reactive power is assumed to be small. The sensitivities of ignored buses need not be negligible, but the optimiser prioritises locations with the higher sensitivities, and only a large enough solution space is to be ensured to find a viable solution.

Shortlisting is performed in each DYNQ iteration using the updated set of BOB–buses. As this set shrinks with each iteration, a fixed search radius selects increasingly fewer candidates. Additionally, some of these candidates may be unavailable if compensation devices were installed there in earlier iterations. To maintain a sufficiently large solution space, the search radius is progressively increased with each iteration, allowing the optimiser to explore a wider electrical neighbourhood to find viable solutions (shown in section IV).

The effectiveness of this reduction depends on the spatial concentration of voltage violations, and is greatest when BOB–buses are concentrated within a smaller region in the grid.

979-8-3315-8138-1

D. Clustering of Candidate Sites

Buses that are electrically close to each other are expected to exhibit similar voltage behaviour. Clustering electrically close buses together allows calculation of sensitivities on only one of them and assign the same to all other buses within the cluster. This reduces simulation effort, albeit at the expense of approximations in sensitivity values.

Hierarchical clustering (implemented with SciPy [14]) is used for clustering, as it allows direct control through distance-based thresholds and better comprehensibility via dendrograms. Other clustering methods, such as K–means and DBSCAN were also tested but were found less suitable due to unequal node densities in the electrical grid and the need for empirical parameter tuning, respectively.

Unlike shortlisting, candidate clustering does not depend on the set of BOB–buses. The clusters are calculated only once for a grid, and does not change for each DYNQ iteration.

III. Simulation Setup

A reduced model of the extra high voltage (EHV) grid of continental Europe projected for 2027 was used. This comprised of a detailed representation of the German 220 kV and 380 kV networks, with the 110 kV aggregated. The neighbouring grids were represented by reduced equivalent models. A single hour of operation was considered, although the DYNQ toolbox is capable of considering multiple operation scenarios. Within this system, only the region of the transmission system operator TenneT TSO GmbH is considered for voltage violations and reactive power planning.

An extensive fault analysis identified four cases representative of all potential TVPI violations across the grid. The target voltage performance is defined in Table I. The violations were observed mainly in the northern and central regions of the grid, with none in the south for the given hour. The faults included three-phase short circuits affecting a single line or a busbar, cleared after 150 ms by taking the respective element out of service. DYNQ was run with the parameters listed in Table II. The system has a total of 105 substations that could be potential candidates to install a compensation device.

IV. Results and Discussion

Results are presented for the baseline, shortlisting, and clustering (combined with shortlisting) cases. Solution quality

TABLE I
Dynamic voltage performance requirements

	τ_{rec}	τ_{dip}	V_{dip}
Voltage thresholds	0.92 pu	0.98 pu	0.98 pu
Target performance	0.3 s	0.3 s	0.02 pu

TABLE II
Parameters used to solve for optimised compensation

Size of test-device for sensitivity calculation	50 Mvar
Max. capacity at candidate location	300 Mvar
(Cost ratio STATCOM : SYNCON)	
Fixed cost of 1×300 Mvar device	1 : 2.2
Size-dependent cost	0.001 : 0.001

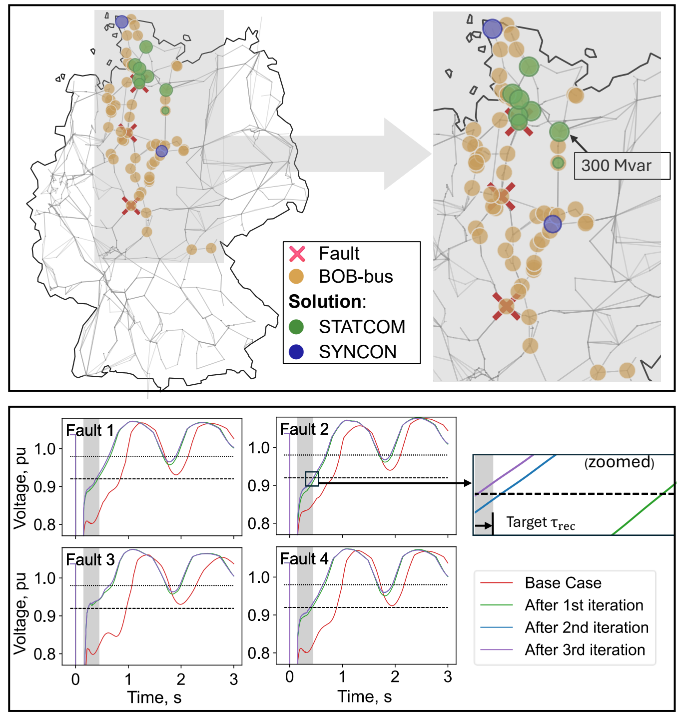

Fig. 4. Baseline results from DYNQ. (top) Fault locations, BOB–buses and optimised reactive power solution, (bottom) Minimum voltage-envelope curves showing TVPI improvement over successive iterations.

is quantified by the total installed reactive power (Total-Q) and the number of STATCOMs and SYNCONs in the solution (STAT/SYN count). With an unchanged device mix, Total-Q is an intuitive proxy for deviation from the brute-force baseline optimum, while the STAT/SYN count reflects practical implementation costs. Computational effort is quantified by the number of RMS simulations and corresponding runtimes tested on 112- and 20-core systems, since DYNQ runs simulations in parallel, and the runtime scales with the available cores.

A. Baseline Results from DYNQ

Fig. 4 shows the fault locations, the BOB–buses, and the optimised reactive power compensation obtained with DYNQ. Further, improvements in short-term voltage behaviour over the iterations are visualised with minimum–envelope curves, that show at any time instant the lowest voltage magnitude observed anywhere in the grid. It can be observed that the first iteration mitigates nearly all violations. Minor deviations attributed to the linearisation assumption of the DYNQ methodology are resolved in successive iterations.

B. Effect of Candidate Shortlisting

An appropriate search radius for candidate shortlisting was determined empirically. For the studied grid, linearly increasing radii of 3, 6, 9, ... Ω gave satisfactory results. The radius was increased over successive iterations as the set of BOB–buses shrank. This is shown in Fig. 5. The shortlisted candidates include the BOB–buses (zero electrical distance to themselves) and additional buses within the search radius.

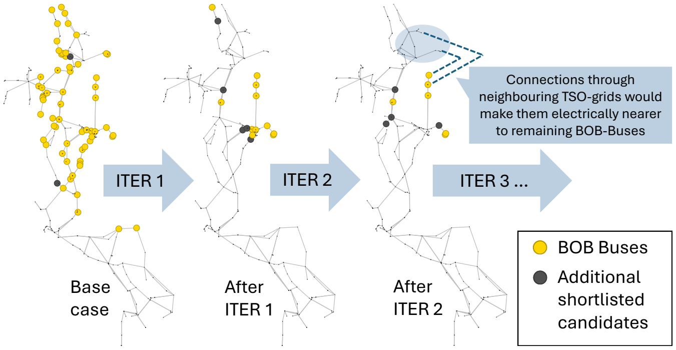

Fig. 5. Dynamic shortlisting of candidate buses around BOB–buses seen over multiple iterations of DYNQ.

A limitation of the current approach was that only the grid-section operated by TenneT was considered. Interconnections through neighbouring grid-sections could slightly alter the computed distances near boundary buses. However, this is not an inherent limitation of the method, since the graph-based distance calculations can similarly be applied on a larger multi-TSO network.

Linearly and exponentially increasing search radii were considered. The DYNQ solutions over successive iterations are compared in Table III. In all configurations, the final solution is largely determined within the first two iterations, which is typical for DYNQ, and is identical across all cases. Minor differences appear only in the third iteration, as buses 6831 and 7488 fall outside the search radius for the linearly increasing case, and bus 6831 also for the exponentially increasing case.

Table IV compares the solution quality and computational performance. Across all cases, Total-Q varies by less than 0.5% with unchanged STAT/SYN count, while computation time is reduced by up to 70% for linearly increasing radii.

TABLE III
DYNQ-RESULTS OVER ITERATIONS WITH CANDIDATE SHORTLISTING

	No shortlist	Shortlist $3, 6, 9\,\Omega$	Shortlist $3, 9, 27\,\Omega$
Iteration 1			
[STATCOM, Bus_735]	300	300	300
[STATCOM, Bus_2435]	250	250	250
[STATCOM, Bus_6939]	300	300	300
[STATCOM, Bus_6998]	300	300	300
[STATCOM, Bus_7098]	300	300	300
[STATCOM, Bus_11032]	124	124	124
[STATCOM, Bus_11084]	300	300	300
[STATCOM, Bus_12087]	300	300	300
[SYNCO, Bus_6831]	295	295	295
Iteration 2			
[SYNCO, Bus_7488]	269	269	269
Iteration 3			
[SYNCO, Bus_6831]	5	–	–
[SYNCO, Bus_7488]	24	–	29
[STATCOM, Bus_11032]	–	40*	–

*Terminated with negligible V_{dip} violations in the order of $10^{-4}pu$.

TABLE IV
DYNQ-PERFORMANCE FOR DIFFERENT SHORTLISTING RADII

	No shortlist	Shortlist $3, 6, 9\,\Omega$	Shortlist $3, 9, 27\,\Omega$
Solution quality			
Total-Q (Mvar)	2767	2779	2768
STAT/SYN count	8/2	8/2	8/2
Performance			
Simulations	$105 + 105 + 105$	$64 + 16 + 10$	$64 + 21 + 65$
Time (h), 112-core	28	8	13
Time (h), 20-core	80	23	38

C. Effect of Candidate Clustering

Fig. 6 illustrates the hierarchical structure of the grid and the resulting clusters with thresholds 2 Ω and 5 Ω. The larger threshold forms bigger, and more number of clusters by combining more distant buses. The effect on the resultant sensitivity matrix is shown in Fig. 7. Here, the sensitivities of

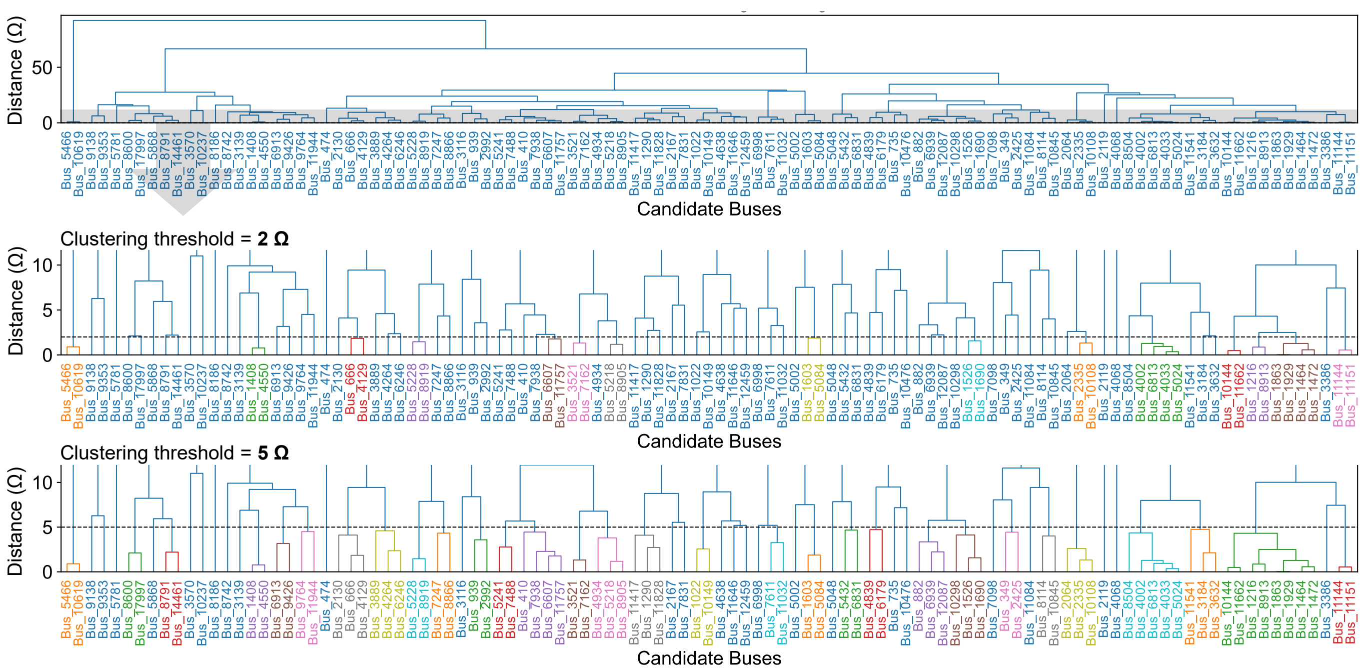

Fig. 6. Dendrogram-based visualization of hierarchical clustering with varying cut-off thresholds.

979-8-3315-8138-1

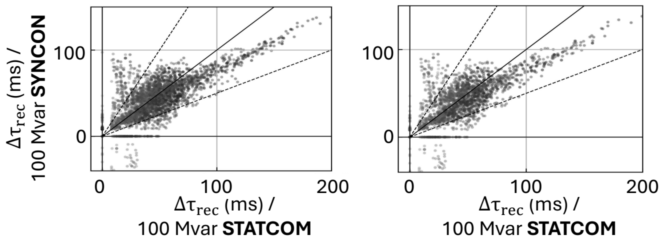

Fig. 7. Sensitivity-scatter for clustering thresholds (left) $2\,\Omega$, (right) $5\,\Omega$.

STATCOMs are plotted against those of SYNCONs, with each point representing a candidate-observed bus pair, for the index τ_{rec} under a single fault case. While both clustering thresholds maintain the same general trends seen in the scatter plot, the density of observed points reduces for the larger threshold. This is expected because we assume larger clusters of nearby buses to have similar sensitivities. Similar results were seen for all indices across all fault cases.

While each method can be applied independently, clustering is applied here on top of shortlisting with linearly increasing radii. The solutions from the two clustering thresholds are compared in Fig. 8, and the accuracy–runtime trade-off is summarised in Table V. With a 2 Ω threshold, the solution is identical to the unclustered case. With 5 Ω, device locations and sizes differ, but Total-Q increases by only about 3.5% with unchanged STAT/SYN count, while simulation time is reduced by about 50% relative to the unclustered case and by about 85% relative to the unclustered, unshortlisted baseline.

The difference in results despite similar total reactive power capacities indicates a relatively flat optimisation problem, i.e., there exist multiple near-optimal solutions. This was also confirmed from the optimiser logs.

V. Conclusion

Seeing the transmission grid as an impedance-weighted graph, this work introduced distance-based preselection of candidate sites for reactive power planning. Applied to the German EHV network within the TenneT control area, solutions comparable to the full brute-force algorithm were produced with greatly reduced computational effort. Relying only on an impedance-weighted representation of the network, the preselection methods are generally applicable to any large-scale interconnected transmission system.

The study demonstrated that electrical distance provides an effective basis for limiting the candidate search space without compromising solution quality. The observed flatness of the optimisation landscape suggests the existence of multiple near-optimal solutions, which is advantageous for practical applications requiring planning flexibility to accommodate additional physical constraints such as limited substation space or site accessibility.

Future work will focus on a more detailed study of sensitivity estimation to further enhance the robustness and applicability of the approach in large-scale system studies. Influencing factors such as load distribution, load modelling, and short-circuit strength, among others, will be examined.

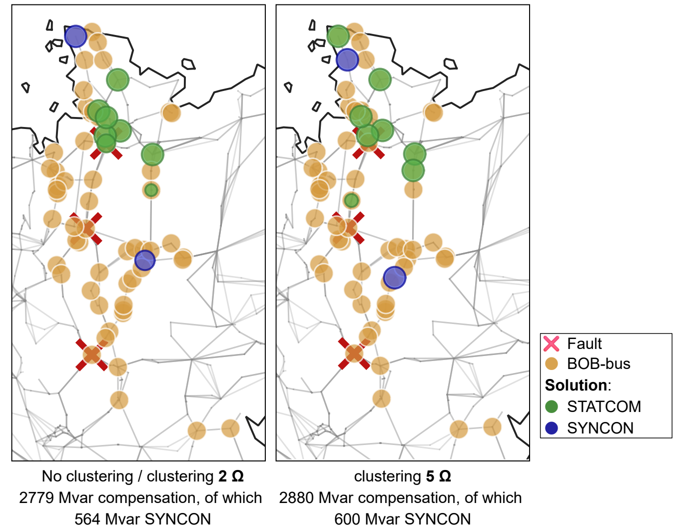

Fig. 8. Comparison of DYNQ solutions with different clustering-thresholds.

TABLE V
DYNQ-Performance with different clustering thresholds

	No clustering	**Clustered $2\,\Omega$**	**Clustered $5\,\Omega$**
Solution quality			
Total-Q (Mvar)	2779*	2779*	2880*
STAT/SYN count	8/2	8/2	8/2
Performance			
Simulations	$64+16+10$	$54+14+9$	$35+9+3$
Time (h), 112-core	8	7	4
Time (h), 20-core	23	20	12

*Terminated with negligible V_{dip} violations in the order of 10^{-4} pu

References

[1] VDE FNN, "Bewertung der systemstabilität: Netzentwicklungsplan strom 2037 mit ausblick 2045, version 2023, zweiter entwurf," tech. rep., VDE Forum Netztechnik/Netzbetrieb (FNN), 2023.

[2] Bundesnetzagentur, "Monitoring report 2022," tech. rep., Bundesnetzagentur, Bonn, Germany, 2022.

[3] I. A. Hiskens and M. Akke, "Analysis of the nordel power grid disturbance of jan. 1, 1997 using trajectory sensitivities," *IEEE Trans. Power Syst.*, vol. 14, no. 3, pp. 987–994, 1999.

[4] B. Sapkota and V. Vittal, "Dynamic var planning in a large power system using trajectory sensitivities," *IEEE Trans. Power Syst.*, vol. 25, no. 1, pp. 461–469, 2010.

[5] A. Tiwari and V. Ajjarapu, "Optimal allocation of dynamic var support using mixed integer dynamic optimization," *IEEE Trans. Power Syst.*, vol. 26, no. 1, pp. 305–314, 2011.

[6] H. Liu, *Planning Reactive Power Control for Transmission Enhancement*. Ph.d. dissertation, Iowa State Univ., 2007.

[7] P. Fakhrooeian, M. Abedi, and P. Karimyan, "Optimal allocation and sizing of dynamic var support to improve short-term voltage stability considering wind farm and dynamic load model," *Int. J. Ind. Electron. Control Optim.*, vol. 1, no. 1, pp. 41–51, 2018.

[8] S. Bose *et al.*, "Reactive power planning in transmission grid considering short-term voltage stability – statcom or syncon?," in *Proc. NEIS Conf.*, 2023.

[9] DIgSILENT GmbH, *PowerFactory*, 2023.

[10] NERC, "Whitepaper on transient voltage response criteria," tech. rep., North American Electric Reliability Corporation, 2022.

[11] A. A. Hagberg, D. A. Schult, and P. J. Swart, "Exploring network structure, dynamics, and function using networkx," in *Proc. 7th Python in Sci. Conf. (SciPy2008)*, pp. 11–15, 2008.

[12] J. J. Grainger and W. D. Stevenson, *Power System Analysis*. New York, NY, USA: McGraw–Hill, 1994.

[13] D. J. Klein and M. Randić, "Resistance distance," *J. Math. Chem.*, vol. 12, no. 1, pp. 81–95, 1993.

[14] P. Virtanen *et al.*, "Scipy 1.0: Fundamental algorithms for scientific computing in python," *Nat. Methods*, vol. 17, pp. 261–272, 2020.

979-8-3315-8138-1